Complex magnetic phenomena
in f-electron intermetallic compounds

A. SZYTUŁA[*]

M. Smoluchowski Institute of Physics, Jagiellonian University, Reymonta 4, 30-059 Cracow, Poland

Various aspects of the magnetic properties of lanthanide and actinide intermetallic compounds are discussed. The first part deals with 1:2:2 stoichiometry compounds. The temperature dependence of magnetic ordering type is discussed. The electronic structures of the investigated compounds are then presented. The third part of the paper concentrates on magnetically hard intermetallics.

Key words: *f-electron intermetallic; magnetic properties; electronic structure*

1. Introduction

During last 25 years, the properties of lanthanide and actinide intermetallics have been extensively investigated from the point of view of both applications and fundamental research. Lanthanides and actinides are representatives of two families that develop the f-electron shell. The physical properties of these compounds deserve vast interest, because of their intriguing fundamental properties resulting from electronic structure and wide applications. The latter reason obviously concerns only lanthanides.

Investigations of lanthanide intermetallics started about four decades ago when lanthanide elements were separated. Neutron diffraction experiments for pure elements indicate complex magnetic structures [1]. Those experimental data led to the development of theoretical models of magnetic interactions in lanthanide metals [2]. Systematic investigations of binary and ternary lanthanide compounds have been performed. These investigations provided lots of new results that were interesting for the fundamental aspects of magnetism, such as crystalline electric field, exchange interactions, magnetoelastic and quadrupolar coupling, etc.

The impact for starting fundamental research on 5f electron materials was doubtlessly the determination of the ferromagnetic properties of UH_3 and UD_3 [3] and the detection of the superconducting state in UBe_{12} [4]. Special attention has been given
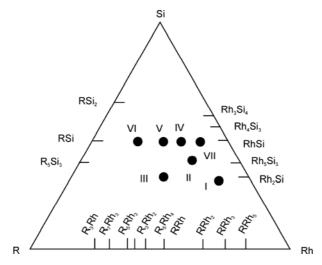
---

[*]E-mail: szytula@if.uj.edu.pl

to ternary compounds. For example, ternary compounds based on transition metals show physical properties different than binary compounds. The synthesis performed using the Pauli paramagnetic compounds CoTi and CoSi results in the strongly ferromagnetic compound Co_2TiSn, with T_C close to room temperature [5].

In the course of investigating the physical properties of binary and ternary lanthanide and uranium phases, a number of new effects have been either discovered or confirmed. Effects such as mixed valence, Kondo lattice spin fluctuations, heavy fermions, and the coexistence of magnetism and superconductivity were found to depend on the electronic structure of lanthanide and uranium ions, in particular they are strongly related to the position of the 4f or 5f electron levels with respect to the Fermi energy. Rare earth intermetallics play an important role in a large part of current research that concerns new magnetostrictive and permanent magnetic materials, spin glass, and random anisotropy systems.

This work concentrates on the magnetic properties of ternary compounds containing 4f electron (rare earth) or 5f electron (actinides) elements (denoted as M), transition metals (denoted as T), and fourth or fifth group elements (denoted as X).

2. Ternary intermetallic

Intermetallic compounds are formed according to the thermodynamic stability of a certain type of crystal structure but quantum chemistry is unable to predict their existence. Phase equilibrium has been investigated only for a small number of possible ternary combinations M–T–X [6]. A typical ternary phase diagram for M–Rh–Si systems (where R is a rare earth element) is shown in Fig. 1. It contains seven phases

Fig. 1. Ternary rare earth–rhodium–silicon phase diagram [6]:
I – RRh_3Si_2, II – RRh_2Si_2, III – $RRhSi$, IV – $R_2Rh_3Si_5$,
V – $RRhSi_2$, VI – R_2RhSi_3, VII – $R_5Rh_4Si_{10}$

with different compositions and crystal structures. The structural, magnetic, and superconducting properties of these systems are summarized in Table 1.

Table 1. Crystallographic, magnetic, and superconductive data of ternary silicides in R–Rh–Si systems[1]

Element	I RRh_3Si_2	II RRh_2Si_2	III $RRhSi$	IV $R_2Rh_3Si_5$	V $RRhSi_2$	VI R_2RhSi_3
	Structure type					
	hexagonal	tetragonal	orthorhombic			hexagonal
	$CeCo_3B_2$ ($P6/mmm$)	$ThCr_2Si_2$ ($I4/mmm$)	NiTiSi ($Pnma$) or cubic ZrOS ($P2_13$)	$Sc_2Co_3Si_5$ ($Ibam$)	$CeNiSi_2$ ($Cmcm$)	($P62c$)
La		S $T_s = 7.4$ K	S $T_s = 4.4$ K	S $T_s = 4.5$ K	S $T_s = 3.4$ K	
Ce		AF $T_N = 36$ K				AF $T_N = 6$ K
Nd	P	AF $T_N = 56$ K		AF $T_N = 2.7$ K		F $T_C = 15$ K
Sm	F $T_C = 34$ K	AF $T_N = 46$ K		P		
Eu		AF $T_N = 25$ K				
Gd	F $T_C = 31$ K	AF $T_N = 98$ K	F $T_C = 18.5$	AF $T_N = 8.4$ K	AF $T_N = 20.5$ K	AF $T_N = 14$ K
Tb	F $T_C = 37$ K	AF $T_N = 94$ K	AF $T_N = 28$ K	AF $T_N = 7.8$		AF $T_N = 11$ K
Dy	F $T_C = 29$ K	AF $T_N = 55$ K	AF $T_N = 14.6$ K	AF $T_N = 4.5$ K		AF $T_N = 6.3$ K
Ho	AF $T_N = 10$ K	AF $T_N = 27$ K	AF $T_N = 8.5$ K	AF $T_N = 2.8$ K		AF $T_N = 5.2$ K
Er	F $T_C = 24$ K	AF $T_N = 12.8$ K	AF $T_N = 8.1$ K	AF $T_N = 2.6$ K		AF $T_N = 5.0$ K

[1] S – superconducor, P – paramagnetic, F – ferromagnetic, AF – antiferromagnetic.

These data and data for other systems indicate that the intermetallic $M_nT_mX_p$ phases have been found to exhibit not only a wide composition range (n:m:p), but also a large variety of crystal structures. The structural characteristics of ternary intermetallic rare-earth compounds were presented in a review paper [7]. Among $M_nT_mX_p$ compounds, only the phases with a 1:2:2 ratio were systematically studied. Based on the data for these systems, the magnetic properties of intermetallic compounds are discussed here. The lanthanide and actinides compounds with a 1:2:2 stoichiometry crystallize in two variants, in a body-centred tetragonal structure (space group $I4/mmm$, $ThCr_2Si_2$ type) or in a primitive tetragonal structure (space group $P4/nmm$, $CaBe_2Ge_2$ type). Both crystal structures are shown in Fig. 2. The atomic framework of both structures can be alternatively displayed as a monatomic sequence perpendicular to the c-axis:

- for the $ThCr_2Si_2$-type structure:

$$R - X - T - X - R - X - T - X - R$$

- and for the $CaBe_2Ge_2$-type structure:

$$R - T - X - T - R - X - T - X - R$$

The layered character and anisotropy ($c/a \approx 2.5$) of the crystal structure of these compounds is strongly reflected in their magnetic properties.
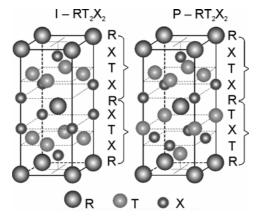

Fig. 2. Crystal structures of MT_2X_2 compounds
of the $ThCr_2Si_2$- and $CaBe_2Ge_2$-type

The results of investigations indicate that the T component carries no magnetic moment in most compounds, except for those with Mn. In MMn_2X_2 (X = Si, Ge) compounds, the Mn moments order at high temperatures, while the rare earth moments usually order antiferromagnetically or ferromagnetically at low temperatures.

Data on the magnetic properties, including magnetic structure, are presented in Refs. [8–11]. In this work, only some data concerning the magnetic ordering of rare earths are presented. The results of neutron diffraction measurements indicate that rare earth sublattices exhibit a large variety of magnetic ordering schemes, including collinear ferro- and antiferromagnetic structures, as well as a number of different non-collinear modulated structures (see Fig. 23 in Ref. [8]). In this work, these structures are briefly discussed as functions of temperature, magnetic field, and pressure.

In some RT_2X_2 compounds, similarly to other rare earth intermetallics, a change in magnetic structure with temperature is observed [12]. For example, in RCo_2X_2 (R = Pr, Nd, Tb, Dy, Ho; X = Si, Ge) the rare earth moments form a collinear antiferromagnetic structure of the AFI type [8]. On increasing temperature, a change in the magnetic structure to a long-period modulated structure is observed (see Table 2). The occurrence of incommensurate phases results from competition between the indirect RKKY exchange, responsible for long-range magnetic ordering, and the crystalline

field anisotropy that might promote uniaxial arrangements. Magnetization as a function of the applied magnetic field gives evidence of phase transitions and new magnetic data. On the basis of these data, the magnetic phase diagram of these compounds is presented (see Fig. 3).

Table 2. Magnetic data for $M_2T_2X_2$ compounds

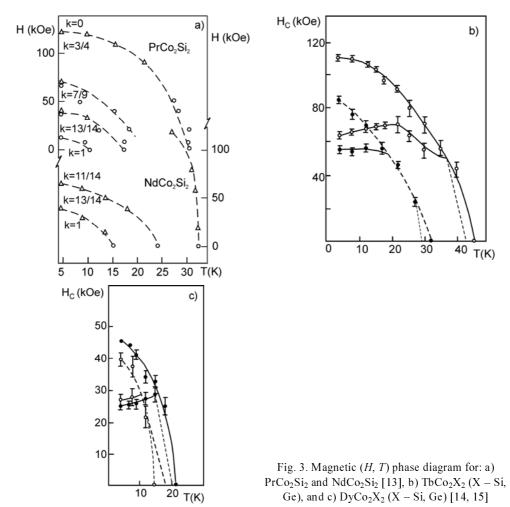| Compound	Magnetic ordering	Reference
$PrCo_2Si_2$	1.5 K < T < 9 K AFI, 9 K < T < 17 K LSWI (k_z = 0.074) 17 K < T < 30 K LSWI (k_z = 0.223)	[a]
$PrCo_2Ge_2$	1.5 K < T < 28 K, LSWI (k_z = 0.27	[b]
$NdCo_2Si_2$	1.5 K < T < 15 K AFI, 15 K < T < 24 K, LSWI (k_z = 0.07), 24 K < T < 32 K LSWI (k_z = 0.20)	[c]
$NdCo_2Ge_2$	1.5 K < T < 12 K AFI, 12 K < T < 28 K LSWI (k_z = 0.261)	[d]
$TbCo_2Si_2$	1.5 K < T < 43.5 K AFI, 43.5 K < T < 45.5 K LSWI (k_z = 0.042)	[e]
$TbCo_2Ge_2$	1.5 K < T < 29.1 K AFI, 29.1 K < T < 34 K LSWI (k_z = 0.055)	[f]
$DyCo_2Si_2$	1.5 K < T < 20.3 K AFI, 20.3 K < T < 21.4 LSWI (k_z = 0.05)	[e]
$DyCo_2Ge_2$	1.5 K < T < 11.5 K AFI, 11.5 K < T < 19.6 K LSWI (k_z = 0.08)	[g]
$HoCo_2Si_2$	1.5 K < T < 14 K AFI	[g]
$HoCo_2Ge_2$	1.5 K < T < 6.7 K AFI, 6.7 K < T < 10.6 K LSWI (k_z = 0.08)	[g]
UNi_2Si_2	1.5 K < T < 53 K LSWI (k_z = ⅓), 53 K < T < 103 K AFI, 103 K < T < 124 K LSWI (k_z = 0.255)	[h]
UNi_2Ge_2	1.5 K < T < 80 K AFI	[i]

AFI – antiferromagnetic collinear structure described by the propagation vector **k** = (0, 0, 1); LSWI – modulated structure described by the propagation vector **k** = (0, 0, 1 – k_z) (see Ref. [9]); [a] Shigeoka T. et al., Physica 156–157 (1989), 741; [b] Pinto H. et al., Acta Cryst. A, 35 (1979), 533. [c] Shigeoka T. et al., J. Phys. (Paris) 49 (1988), C8-431; [d] André G. et al., J. Magn. Magn. Mater., 86 (1990) 387; [e] Szytuła A. et al., J. Phys.: Cond. Matter, 12 (2000), 7455; [f] Penc B. et al., J. Phys.: Cond. Matter, 11 (1999), 7579; [g] Schobinger-Papamantellos P. et al., J. Magn. Magn. Mater., 264 (2003), 130; [h] Rebelsky L. et al., Physica B, 180–181 (1992), 43; [i] Chełmicki L. et al., J. Phys. Chem. Solids, 46 (1985), 528.

The interpretation of such magnetic behaviour is possible on the basis of various theoretical models: the ANNNI (anisotropic-next-nearest-neighbour-Ising) model [16], Date's incommensurate mean field model [17], or self-consistent periodic field model [18]. All these models reproduce the observed change in magnetic structure as a function of temperature or magnetic field.

The $PrNi_2Si_2$ system exhibits the most original behaviour. Pr magnetic moments form an amplitude-modulated structure down to 0 K. At low temperature, squaring to the antiphase structure was detected. The external magnetic field causes a change in the ferromagnetic state. The above results indicate that the ground state is nonmagnetic [11].
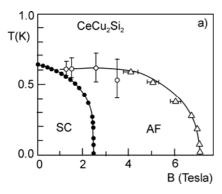
Anomalous properties are observed in some 1:2:2 compounds with R = Ce, Eu, Yb. The temperature dependence of specific heat indicates that $CeCu_2Si_2$ is a superconductor below 0.5 K. The large value of the electric specific heat (γ = 1.1 J/(mol·K^2)) suggests that $CeCu_2Si_2$ is a heavy fermion system with an effective mass of approximately 100m_0

[19]. The external magnetic field causes the superconducting state to disappear and induces an antiferromagnetic one [20]. The phase diagram of $CeCu_2Si_2$ is presented in Fig. 4a. A different effect is observed in $CePb_3$, in which the external magnetic field induces the superconducting state (see Fig. 4b) [21].

Fig. 3. Magnetic (H, T) phase diagram for: a) $PrCo_2Si_2$ and $NdCo_2Si_2$ [13], b) $TbCo_2X_2$ (X – Si, Ge), and c) $DyCo_2X_2$ (X – Si, Ge) [14, 15]

$CePd_2Si_2$ is an antiferromagnet with the Néel temperature T_N equal to 10 K and collinear magnetic structure described by the propagation vector $\mathbf{k} = (1/2, 1/2, 0)$ [22]. The temperature dependence of electrical resistivity ρ as a function of external pressure, summarized in Fig. 5a, indicates the following:

- the Néel temperature T_N decreases slowly and monotonically with increasing pressure,
- at a critical pressure P_c of ~26 kbar, the phase transition to the superconducting state takes place.
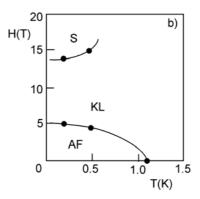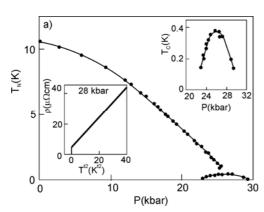
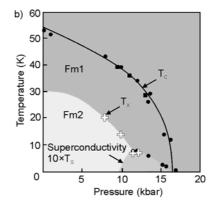Fig. 4. Magnetic (H, T) phase diagram of: a) $CeCu_2Si_2$ [20], b) $CePb_3$ [21]

Fig. 5. T, p phase diagrams of: a) $CePd_2Si_2$ [23, 24], b) UGa_2 [28]

It was observed that ρ changes as $T^{1.2(1)}$ near P_c, which is indicative of non-Fermi behaviour. The behaviour of $\rho(T)$ and $T_N(P)$ near P_c suggests that spin fluctuations have a 2D character [19, 20].

The 1:2:2 uranium compounds show similar properties to those of isostructural rare earth compounds. The most interesting discovery for these compounds, however, was their heavy-fermion behaviour, at first in URu_2Si_2 ($\gamma = 180$ mJ/(mol·K^2)) [25]. Neutron diffraction studies confirmed that URu_2Si_2 exhibits an AFI-type magnetic structure below 17 K, with a very small magnetic moment of 0.04(1)μ_B at $T = 0.57$ K [26]. At low temperatures, below 1 K, a transition to a superconducting state was detected [27].

UGe_2 compounds are ferromagnets with the Curie temperature T_C of 52 K for which an external pressure P causes monotonical decrease of T_C, and at about P = 1 GPa induces the superconducting state (Fig. 5b) [28].

EuT_2X_2 compounds are the most suitable for studying valence fluctuations, for example by ^{151}Eu Mössbauer spectroscopy, because the isomer shift has significantly different values for Eu^{2+} ($\delta_{IS} = -10.6$ mm/s) and Eu^{3+} ($\delta_{IS} = 0.6$ mm/s) ions. Figure 6 shows the classification of silicides and germanides based on the isomer shift and

atomic volumes at room temperature. In germanides Eu ions are trivalent which is associated with the large volume available for Eu^{3+} ions in the unit cell. The case of silicides is much more complex: depending on the volume of the unit cell, Eu^{2+}, Eu^{3+} ions or mixed-valence states are present. It was estimated that the fluctuation time between the two valence states is shorter (10^{-13} s) than the Mössbauer probe time (10^{-11} s). Germanides (EuT_2Ge_2 for T = Co, Ni, Cu, Ru and Rh) are antiferromagnets, while only silicides, EuT_2Si_2, with T = Ru, Rh, Ag, and Au are antiferromagnets [10, 28].

Fig. 6. Parameters of EuT_2Si_2 (left panel) and EuT_2Ge_2 (right panel) at 300 K: the unit cell volume in $Å^3$ (upper right), isomer shift in mm/s of the ^{151}Eu Mössbauer absorption (bottom left) and valence (bottom right) for various T elements

Magnetic data have been published only for some YbT_2X_2 phases (see Ref. [10]). The majority of these compounds exhibit an unstable 4f shell intermediate valence effect. In contrast to the compounds with Ce and Eu, in the case of Yb the mixed-valence state is observed for both silicides and germanides. Lately, the magnetic properties of $YbRh_2Si_2$, which is a weak antiferromagnet below $T_N = 70$ mK [30] have been determined. The magnetic phase diagram (see Fig. 5 in Ref. [30]) indicates complex magnetic and electronic properties. In this diagram, antiferromagnetic (AF), non-Fermi liquid (NFL) and Landau-Fermi liquid phases exist.

RMn_2X_2 (X = Si, Ge) compounds exhibit two critical temperatures [31]:

• at low temperatures the magnetic moments are localized on the R atoms and become ordered,

• at high temperatures only magnetic moments on Mn atoms show either ferro- or antiferromagnetic ordering.

The type of magnetic ordering in the Mn sublattice depends on the interatomic Mn–Mn distance. The coupling between Mn–Mn moments is antiferromagnetic when $R^a_{Mn-Mn} < 0.285$ nm and becomes ferromagnetic for $R^a_{Mn-Mn} > 0.285$ nm [32]. Similar critical distances were observed in many other alloys with transition metals [33]. The localization-delocalisation effect of 3d electrons occurs when the critical distance in Mn compounds reaches 0.285 nm [34].

$SmMn_2Ge_2$ has interesting magnetic properties – in the temperature range 341 K < T < 385 K it is antiferromagnetic, but ferromagnetic in the range 153 K < T < 341 K. It becomes a re-entrant antiferro- (106.5–153 K) and ferromagnetic below 106.5 K [35, 36]. External pressure changes these magnetic phase transitions [30]. The fact that

in the antiferromagnetic state the resistance is higher than in the ferromagnetic state suggests the giant magnetoresistance in this compound [37]. Extraordinary large changes of magnetoresistance during metamagnetic phase transitions in TbNiSn single crystals at 4.2 K were observed [38].

3. Frustration systems

Geometrically frustrated systems are ubiquitous and interesting because their behaviour is difficult to predict as frustration can lead to a macroscopic degeneracy and qualitatively new states of matter.
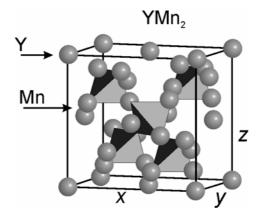

Fig. 7. The cubic corner-sharing tetrahedron lattice
        and crystal structure of YMn_2

The fundamental unit of frustration is a system of three antiferromagnetically interacting spins on a regular triangle. A regular tetrahedron composed of four triangles serves as a unit of three-dimensional frustrated lattices. Geometrically frustrated lattices are formed by joining their edges or corners. The triangular lattice and face-centered cubic lattice are edge-sharing lattices of triangles and tetrahedrons, respectively. Corner-sharing triangles yield the kagomé lattice while tetrahedrons form the lattice presented in Fig. 7. A number of magnetic materials crystallize in the last type of structure which belong to different classes of crystal symmetries, such as normal spinel, pyrochlores ($Y_2Mo_2O_7$). and $C15$ Laves phase intermetallic compounds such as Y(Sc)Mn$_2$. In all these systems, the Mn magnetic ions form corner-shared tetrahedrons as depicted in Fig. 7. As in the case of the two-dimensional triangular lattice, this topology leads to a highly frustrated lattice, in which magnetic interactions between Mn moments are negative. Moreover, Mn moments in the RMn$_2$ series are very close to the magnetic-nonmagnetic instability as a function of distance. The critical distance is $d_c = 2.66$ Å. It has been determined that a complex magnetic structure arises as a result of frustration in YMn$_2$, with a long wavelength distorted helical component [39].

A large group of the rare earth intermetallics crystallize in the hexagonal ZrNiAl -type structure (space group $P\bar{6}2m$). The distribution of rare earth atoms in the basal

plane is similar to that in the kagomé lattice (Fig. 8). The results of neutron diffraction measurements indicate the existence of complex magnetic structures in these compounds. For example, in TbAuIn the Tb moments in the *ab* plane form a typical triangle structure (Fig. 9) [40]. A similar magnetic ordering is observed in a large number of isostructural compounds [41].
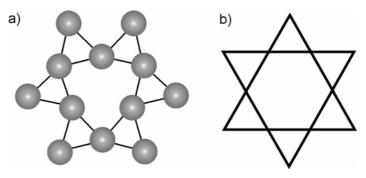

Fig. 8. Projection of the hexagonal ZrNiAl-type structure on the basal plane (a). Only rare earth atoms are shown, kagomé lattice (b)
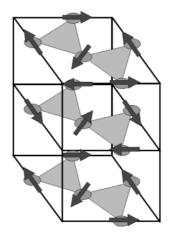

Fig. 9. Typical magnetic structure observed in RTX compounds with a ZrNiAl-type crystal structure

4. Electronic structure

Knowledge of the band structure of MT_2X_2 should lead to a better understanding of their magnetic properties. Results of X-ray absorption spectroscopy and XPS studies carried out on CeT_2Si_2 compounds (T = 3d metal) indicate that with an increasing number of 3d electrons per atom the maximum of the 3d band moves below the Fermi level (Fig. 10) [42, 43]. For Mn compounds the Mn 3d states are at the Fermi level. With an increasing number of 3d electrons, the peak corresponding to the T 3d state moves away from the Fermi level. Calculations performed for YMn_2Ge_2, $LaMn_2Ge_2$, $LaCo_2Ge_2$

[44], YMn_2Si_2, $LaMn_2Si_2$ [45] and $YbMn_2Si_2$ and $YbMn_2Ge_2$ [46] indicate that the Fermi level crosses the 3d band. The calculated density of states at the Fermi level $N(E_F)$ is equal to 1.47 states/(eV·atom) for YMn_2Si_2, 1.78 for $LaMn_2Si_2$ [45], 1.47 for YMn_2Ge_2 and 2.13 for $LaMn_2Ge_2$ [44], 4.10 for $YbMn_2Si_2$ and 2.97 for $YbMn_2Ge_2$ [46], and 0.6 for $LaCo_2Ge_2$. The last value implies that the Co 3d band in $LaCo_2Ge_2$ is located below the Fermi level [44]. XPS spectra of the valence band of $HoFe_2Ge_2$ (see Fig. 11) indicate that the valence band is dominated by the multiplet structure of Ho^{3+}. Near the Fermi level, a broad maximum corresponding to Fe 3d states is observed.
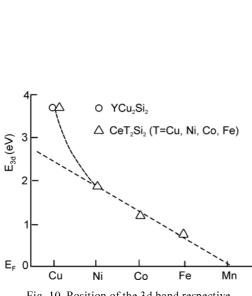

Fig. 10. Position of the 3d band respective to the Fermi level in CeT_2Si_2 (T – Cu, Ni, Co, Fe) [42] and YCu_2Si_2 [43]
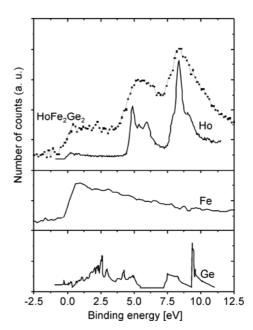

Fig. 11. XPS spectra of the valence band of $HoFe_2Ge_2$ and pure Ho, Fe, and Ge elements

The calculated band structures of $CeCu_2Si_2$ and $LaCu_2Si_2$ show that the 4f levels of Ce are located mainly above E_F. The density of states at E_F is large. The XPS spectra obtained for CeT_2Si_2 (T = Cu, Ag, Au, Pd) suggest that the hybridisation of the 4f electrons of Ce with the d-states of T ions takes place [47].

An analysis of the XPS spectra of Ce $3d_{5/2}$ and Ce $3d_{3/2}$ states based on the Gunnarsson–Schönhammer model determined the hybridisation energy of the Ce 4f orbital with the conduction band to be 59 meV [48] for $CeCu_2Si_2$ and 220 meV for CeT_2X_2 (T = Ni, Cu; X = Sb, Sn) [49].

The electronic structure of UT_2Si_2 (T = Ru, Rh, Pd, Ir) was determined by means of XPS measurements [50] and calculation of the density of states [51]. The situation in the valence band of uranium intermetallic compounds can be characterized by a more or less narrow 5f band intersected at the Fermi level. The XPS spectra of

UT_2Si_2 (T = Ru, Rh, Pd, Ir) [50] indicate that the structure of the Fermi surface is formed by the 5f states of uranium. For the 4d states of the transition metal a shift of the centre of the d-band from 1.9 eV for Ru to 3.9 eV for Pd is observed. These data indicate that for URu_2Si_2 a strong hybridisation of the U 5f and Ru 4d states appears to be very close to nonmagnetic-magnetic instability.

5. Magnetic hard materials

Historically, the trend in the development of permanent magnets is to rapidly increase $(BH)_{max}$ (Fig. 11). Impressive progress in these materials was observed during the 20th century. Progress in new hard materials with large $(BH)_{max}$ values, which gives the maximum energy product of the magnet, was obtained for rare earth–3d intermetallics. The interesting magnetic properties of these materials result from different microscopic magnetic properties of the elements. The rare earth atoms, with 4f electrons, display localized magnetic moments. On the contrary, the 3d-electrons of the transition metals are considered to be itinerant. On the basis these materials, new materials for permanent magnets are obtained, first the system R–Co with 1:5 and 2:17 stoichiometries [52], and next the $Nd_2Fe_{14}B$ compound with a relatively large T_C equal to 589 K and very large value of $(BH)_{max}$ (50 MGOe) [53, 54].

Fig. 12. Evolution of the maximum energy product of permanent magnets during the 20th century

The next group of compounds, which have been proposed as cheap alternative materials for the production of permanent magnets, are $RT_{12-x}T'_x$ compounds, where R is a rare earth element, T is a 3d electron element, T′ is Ti, V, Cr, Mn, Mo, W, Al, or Si, and x is in the range $1 < x < 4$ [55]. These compounds have Curie temperatures ranging

from 260 to 650 K, with the highest values for Gd compounds in each series, except for the Mo-containing series, for which the maximum occurs for the Sm compound. $RFe_{12-x}M_x$ compounds are characterized by high Curie temperatures and high uniaxial anisotropy, and are good materials for the production of permanent magnets. In order to obtain the best parameters of these compounds, light elements such as H, C, and N are used and they have a dramatic effect on the magnetic properties (see Table 3).

Table 3. Main characteristics as observed after interstitial charging of hard magnetic compounds[*]

Quantity	Compound			
	R_2Fe_{17}		$RFe_{12-x}M_x$	
Interstitial	H	C, N	H	C, N
Curie temperature T_C	ii	iii	ii	iii
Saturation magnetization M_s	i or c	i	ii	
Anisotropy fields H_A	d or c	iii	i or c	

[*]d – decrease, c – constant, i – increase, ii – large increase, iii – very large increase.

6. Conclusions

The analysis of the structural and magnetic ternary intermetallic phases enables a number of general conclusions to be drawn. The first characteristic feature is the existence of many phases in each of these ternary systems, having different magnetic properties. The magnetic properties of the different intermetallics presented in this work indicate that these properties are strongly correlated with the electronic states of atoms. In the discussed compounds, the "normal" lanthanide and uranium atoms have localized magnetic moments. The localization of magnetic moments on 3d-electron atoms depends on the concentration of these atoms in the compound. For high concentrations of iron, the magnetic moment is localized, while for low concentrations (except for Mn) the magnetic moments of 3d-electron atoms disappear. The magnitude of the magnetic moment μ of 3d-electron atoms is proportional to the distribution of the bands of spin up and spin down electrons.

In 1:2:2 type intermetallic compounds, the magnetism arises from the interaction of magnetic moments localized on f-electron ions. The magnetic order observed in these compounds results from a compromise between different interactions and thermal effects. These interactions are of two types. The first, the bilinear exchange interaction of the RKKY type, is long range, oscillates with distance, and leads to different magnetic structures. It is also incommensurate with the crystallographic lattice. The second interaction to be taken into account is the crystalline electric field (CEF). In an uniaxial structure, CEF favours Ising and X–Y systems, with magnetic moments parallel and perpendicular to the tetragonal c-axis, respectively.

References

[1] Koehler W.C., [in:] *Magnetic Properties of Rare Earth Metals*, R.J. Elliott (Ed.), Plenum Press, New York, 1972.

[2] Kasuya T. Prog. Theor. Phys., (Kyoto) 16 (1956), 45; Ruderman M.A., Kittel C., Phys. Rev., 96 (1954), 93.

[3] Trzebiatowski W., Śliwa A., Staliński B., Roczn. Chemii, 26 (1952), 110; ibid 28 (1954), 12.

[4] Maple M.B., Chen J.W., Lambert S.E., Fisk Z., Smith J.L., Ott H.R., Brooks J.S., Naughton M.J., Phys. Rev. Lett., 54 (1985), 477.

[5] Fujita Y., Endo K., Terada M., Kimura R., J. Phys. Chem. Solids, 33 (1972), 1443.

[6] Chevalier B., Leyay P., Etourneau J., Hagenmuller P., Matter. Res. Bull., 18 (1983), 315.

[7] Bodak O.I., Gladyshevsky E.I., [in:] *Handbook on the Physics and Chemistry of Rare Earths*, Vol. 13, K.A. Gschneidner Jt., L. Eyring (Eds.), North Holland, Amsterdam 1990, 1.

[8] Szytuła A., Leciejewicz J., [in:] *Handbook on the Physics and Chemistry of Rare Earths*, Vol. 12, KA. Gschneidner Jr., L. Eyring (Eds.), Elsevier Science Publ. B.V., 1989, p. 133.

[9] Szytuła A., [in:] *Handbook of Magnetic Materials*, Vol. 6, H.H.J. Buschow (Ed.), Elsevier, 1991, p. 85.

[10] Szytuła A., Leciejewicz J., *Handbook of Crystal Structures and Magnetic Porperties of Rare Earth Intermetallics*, CRC Press, Boca Raton, 1994.

[11] Gignoux D., Schmitt D., [in:] *Handbook on the Physics and Chemistry of Rare Earths*, Vol. 20, K.A. Gschneidner Jr., L. Eyring (Eds.), Elsevier, p. 293.

[12] Gignoux D., Schmitt D., Phys. Rev. B, 48 (1993), 12682.

[13] Vinokurova L., Ivanov V., Szytuła A., J. Magn. Magn. Mater., 99 (1991), 193.

[14] Vinokurova L., Ivanov V., Szytuła A., J. Alloys Comp., 190 (1992), L23.

[15] Shigeoka I., Garnier A., Gignoux D., Schmitt D., Zhang F.Y., Burlt P., J. Phys. Soc., Japan, 63 (1994), 2731.

[16] Bak P., Von Boehm J., Phys. Rev. B, 21 (1980), 5297.

[17] Date M., J. Phys. Soc., Japan, 57 (1988), 3682.

[18] Iwata N., J. Magn. Magn. Mater., 86 (1990), 225.

[19] Stewart G.R., Rev. Mod. Phys., 56 (1984), 755.

[20] Nakamura H., Kitaoka Y., Yamada H., Asayama K., J. Magn. Magn. Mater., 76–77 (1988), 517.

[21] Lin C.L., Teter J., Crow J.E., Mihalisin T., Brooks J., Abou-Aly A.I., Stewart G.R., Phys. Rev. Lett., 54 (1985), 2541.

[22] Steeman R.A., Frikkee E., Helmholdtr B., Menovsky J., Vandenberg J., Nieuwenhuys G.J., Mydosh J.A., Solid State Commun., 66 (1988), 103.

[23] Julian S.R., Carter F.V., Grosche F.M., Haselwimmer R.K.W., Lister S.J., Mathur N.D., Mcmullan G.J., Pfeleiderer C., Saxena S.S., Walker I.R., Wilson N.J.W., Lonzarich G.G., J. Magn. Magn. Mater., 177–181 (1998), 265.

[24] Mathur N.D., Grosche F.M., Julian S.R., Walker I.R., Freye D.M., Haselwimmer R.K.W., Lonzarich G.G., Nature, 394 (1998), 39.

[25] Schlabitz W., Bauman J., Pollit B., Rauchschwelbe U., Mayer H.M., Ahleheim U., Bredl C.D., Z. Phys. B, 62 (1986), 171.

[26] Broholm C., Kjems J.K., Buyers W.J.L., Matthew P., Palstra T.T.M., Menovsky A.A., Mydosh J.A., Phys. Rev. Lett., 58 (1987), 1467.

[27] Lopez De La Torre M.A., Visani P., Dalichaouch Y., Lee B.W., Maple M.B., Physica B, 179 (1992), 208.

[28] Saxena S.S., Agarval P., Ahilan K., Grosche F.M., Haselwimmer R.K.W., Steiner M.J., Pugh E., Walker L.B., Julian S.R., Monthoux P., Lonzarich G.G., Huxley A., Shelkin L., Braithwaite D., Flouquet J., Nature, 106 (2000), 587.

[29] Görlich E.A., Ph. D. Thesis, Jagiellonian Univeristy, Cracow, 1997.

[30] GEGENWART P., CUSTERS J., TAYAMA T., TENYA K., GEIBEL C., TROVARELLI O., STEGLICH F., Acta Phys. Polon., 34 (2003), 323.

[31] SZYTUŁA A., SZOTT I., Solid State Commun., 40 (1981), 199.

[32] SZYTUŁA A., SIEK S., J. Magn. Magn. Mater., 27 (1982), 49.

[33] FORRER R., Ann. Phys., 7 (1952), 605.

[34] GOODENOUGH J.B., *Magnetism and Chemical Bond*, Wiley, New York, 1963, p. 240.

[35] DURAJ M., DURAJ R., SZYTUŁA A., TOMKOWICZ Z., J. Magn. Magn. Mater., 73 (1988), 240.

[36] GYORGY E.M., BATLOGG B., REMEIKA J.P., VAN DOVER R.B., FLEMING R.M., BAIR H.E., ESPINOSA G.P., COOPER A.S., MAINES R.G., J. Appl. Phys., 61 (1987), 4237.

[37] BRABERS J.H.V.J., NOLTEN A.J., KAYZEL F., LENCZOWSKI S.H.J., BUSCHOW K.H.J., DEBOER F.R., Phys. Rev. B, 50 (1994), 16410.

[38] HORI H., OKI A., KURISU M., FURUSAWA M., ANDOH Y., KINDO K., Phys. Lett. A, 224 (1997), 293.

[39] BALLOU R., DEPORTES J., LEMAIRE R., NAKAMURA Y., OULADDIAF B., J. Magn. Magn. Mater., 70 (1987), 129.

[40] SZYTUŁA A., BAŻELA W., GONDEK Ł., JAWORSKA-GOŁĄB T., PENC B., STÜSSER N., ZYGMUNT A., J. Alloys Comp., 336 (2002), 11-17.

[41] GONDEK Ł., Ph. D. Thesis, Jagiellonian University, Cracow, 2004.

[42] SAMPATHKUMARAN E.V., KALKOWSKI G., LAUBSCHAT C., KAINDL G., DOMKE M., SCHMIESTER G., WORTMANN G., J. Magn. Magn. Mater., 47–48 (1985), 212.

[43] BUSCHOW K.H.J., CAMPAGNA M., WARTHEIM S.K., Solid State Commun., 24 (1977), 253.

[44] ISHIDA S., ASANO S., ISCHIDA J., J. Phys. Soc. Jpn., 55 (1986), 93.

[45] KULATOV E., VESELAGO V., VINOKUROVA L., Acta Phys. Polon., A 77 (1990), 709.

[46] SZYTUŁA A., JEZIERSKI A., PENC B., HOFMANN M., CAMPBELL S.J., J. Alloys Comp., 366 (2004), 313.

[47] PARKS R.D., REHL B., MERTENSSON N., STEGLICH F., Phys. Rev. B, 27 (1983), 6052.

[48] KANG J.S., ALLEN J.W., GUNARSSON O., CHRISTENSEN N.E., ANDERSEN O.K., LASSAILLY Y., MAPLE M.B., TORIKACHVILI M.S., Phys. Rev. B, 41 (1990), 6610.

[49] ŚLEBARSKI A., JEZIERSKI A., ZYGMUNT A., NEUMANN M., MÄHL S., BORSTEL G., J. Magn. Magn. Mater., 159 (1996), 179.

[50] GRASSMANN A., Physica B, 163 (1990), 547.

[51] SANDRATSKII L.M., KUBLER J., Solid State Commun., 91 (1994), 183.

[52] STRNAT K.J., HOFFER G., OLSON J., OSTERTAG W., BECKER J.J., J. Appl. Phys., 38 (1967), 1001.

[53] SAGAWA M., FUJIMURA S., TOGAWA N., YAMAMOTO H., MASUURA Y., J. Appl. Phys., 55 (1984), 2083.

[54] CROAT J.J., HERBST J.F., LEE R.W., PINKERTON F.E., Appl. Phys. Lett., 44 (1984), 148.

[55] SUSKI W., [in:] *Handbook on the Physics and Chemistry of Rare Earths*, Vol. 22, K.A. Gschneidner Jr., L. Eyring (Eds.), Elsevier, Amsterdam, 1996.